Copernicus Marine Service

SYNTHESIS QUALITY DOCUMENT

SYNTHESIS QUALITY OVERVIEW DOCUMENT (SQO)

Associated to extended quality information document (QUID): CMEMS-MED-QUID-006-014

QUID Version: 3.1

Associated to Product ID:

MEDSEA_ANALYSISFORECAST_BGC_006_014

Issue: 3.1

Contributors to SQO: L. Feudale, A. Teruzzi, S. Salon, G. Bolzon, P. Lazzari, G. Coidessa, V. Di Biagio, E. Alvarez, C. Amadio, G. Cossarini

SQO approval date by the CMEMS PQ coordination team: 12/01/2024

CHANGE RECORD

When the quality of the products changes, the QuID is updated and the SQO is updated. A line is added to this table and the version of the SQO document is the same than that of the REFERENCE QUID. The third column specifies which sections or sub-sections have been updated.

Issue	Date	§	Description of Change	Authors	Validated By
2.0	15/01/2021	All	Creation of the document	L. Feudale, A. Teruzzi, S. Salon, G. Bolzon, P. Lazzari, G. Coidessa, V. Di Biagio, G. Cossarini	Emanuela Clementi (Med-MFC Deputy Leader)
2.1	03/03/2021	All	Release of version Q4/2021 of the Med-biogeochemistry with the addition of the daily discharges of nutrients and carbonate system variables for the Po River (Adriatic Sea)	L. Feudale, A. Teruzzi, S. Salon, G. Bolzon, P. Lazzari, G. Coidessa, V. Di Biagio, G. Cossarini	Emanuela Clementi (Med-MFC Deputy Leader)
3.0	31/08/2022	All	Release of version Q4/2022 of the Med-biogeochemistry with the new optical component (OASIM atmospheric irradiance model and new BFM with multispectral radiative component) and assimilation of Argo oxygen	L. Feudale, A. Teruzzi, S. Salon, G. Bolzon, P. Lazzari, G. Coidessa, Di Biagio V., E.Alvarez, C. Amadio, G. Cossarini	Anna Chiara Goglio (Med-PQ Responsible)
3.1	16/06/2023	All	Release of version Q4/2023 of the Med-biogeochemistry with tuning of the bio-optical component and addition of PFTs chlorophyll and carbon biomass of 4 Phytoplankton Functional Types	L. Feudale, A. Teruzzi, S. Salon, G. Bolzon, P. Lazzari, G. Coidessa, Di Biagio V., E. Álvarez, C. Amadio, G. Cossarini	Anna Chiara Goglio (Med-MFC PQ Responsible)

Contents

Executive summary

The quality of the Mediterranean Sea biogeochemistry analysis and forecasts product has been assessed for the year 2019 by means of comparison with observational in-situ datasets, semi-independent data (satellite and BGC-Argo float used in the assimilation) and literature estimates:

Chlorophyll: Results give evidence of the model capability of reproducing spatial patterns, seasonal cycle with surface winter bloom period, and vertical dynamics at mesoscale and weekly temporal scale.

Primary production: Comparison has been made with available peer-reviewed publications, showing that the simulation consistently reproduces basin-scale and sub-basin-scale patterns and estimates.

Phytoplankton carbon biomass: The 0-200 m averaged values are reproduced with an accuracy of around 1.3 mgC/m^3 considering BGC-Argo bbp700 optical data converted to carbon biomass.

Zooplankton carbon biomass: The 0-200 m integrated values are compared with few sparse estimations retrieved from literature: model consistently reproduces the order of magnitude of this variable.

Phosphate: General basin-wide gradients and vertical profile shapes are simulated consistently with respect to observations: mean monthly vertical profiles are within the observed climatological variability.

Nitrate: Horizontal spatial gradients and vertical patterns are consistent with observations. Mean monthly vertical profiles are within the observed climatological variability but a possible surface overestimation in western subbasins and deeper layer underestimation in the eastern basin are noticed. Consistency of mesoscale vertical dynamics is confirmed by the comparison with BGC-Argo float data.

Oxygen: Model profiles are in agreement with climatology and generally within the observed variability. Model outputs consistently reproduce the oxygen weekly dynamics at the mesoscale and its vertical patterns according to the comparison with BGC-Argo data.

Ammonium: Results are affected by the low data availability. The order of magnitude is captured, but the horizontal patterns and the vertical variability are not always well reproduced.

Silicate: Basin averaged vertical profiles are within the range of variability of the climatology except in the western basins where the model overestimates concentration at the surface.

pH: Uncertainty of modelled pH in total scale is 0.020 according to the comparison with reconstructed climatological vertical profiles.

Alkalinity: Considering the comparison of model results with climatological vertical profiles, the basin-scale uncertainty of Alkalinity is around 19 µmol kg^{-1}.

Dissolved inorganic carbon (DIC): Considering the comparison of model results with climatological vertical profiles, the basin-scale uncertainty of DIC is around 18 µmol kg^{-1}.

Surface partial pressure of CO_2 (pCO2): The model values show good agreement with the observed seasonal cycle and spatial heterogeneity among sub-basins.

Flux of CO_2 at the air-sea interface: Present CO_2 flux estimates are consistent with a multi-decadal reanalysis climatology and literature estimations.

Light attenuation Coefficient at 490nm wavelength (Kd490): it is computed for the surface layer (first optical depth) and it is provided in m^{-1} unit. Comparison with Ocean Color data

verifies the good performances of the model in coastal and open sea areas in winter and summer seasons.

For additional information regarding the in-depth validation of this product, the calculation of the assessment metrics presented in this product other detailed information in quality and noticeable events please refer to the reference QuID document CMEMS-MED-SQO-006_014.

Important notice:

The contents of this document are an assessment based on the best set of observations available for evaluation at the time the operational system was validated. The validation methodology was defined and agreed within Marine Copernicus, inheriting the long experience of MyOcean and MERSEA series of projects (Hernandez et al., 2018), the results presented in this report and derived estimated accuracy numbers (EAN) are representative of average error levels over large areas of the ocean. These numbers might be used as a mean error of the product, while to refine error estimates locally, the reader is invited to use complementary information from the reference QUIDs (error maps for instance, when available).

1. Chlorophyll

Results give evidence of the model capability of reproducing spatial patterns, seasonal cycle with surface winter bloom period, and the related vertical properties at mesoscale and weekly temporal scale. The comparison over 2019 with satellite observations at surface shows that the western open sea sub-basins are generally characterized by higher uncertainty and variability (estimated by the RMSD) than eastern ones, with a basin-averaged RMSD of 0.05 (0.01) mg m^{-3} in winter (summer). In the coastal areas, the basin-averaged uncertainty rises up to 0.23 (0.19) mg m^{-3} in winter (summer), with higher values in areas more affected by river inputs and shelf dynamics, and a general model underestimation of the high values of observed chlorophyll. The use of the available BGC-Argo floats data shows model consistency in reproducing the key mechanisms coupling physics and biogeochemistry at mesoscale and along the vertical dynamics. The mean RMSD between model and BGC-Argo observations in the 0-150m layer is 0.04 mg m^{-3}. Further, the model skill in reproducing vertical processes assed with some novel metrics: averaged content of chlorophyll in the photic layer (0-200 m), depth of Deep Chlorophyll Maximum (DCM) and thickness of the winter bloom layer (WBL). Considering areas with a sufficient number of float profiles, the modelled averaged content of chlorophyll in the photic layer (0-200 m) has a mean RMSD of 0.06 mg m^{-3}, the DCM is reproduced with an uncertainty of around 8 m, while WBL has an uncertainty of 27 m.

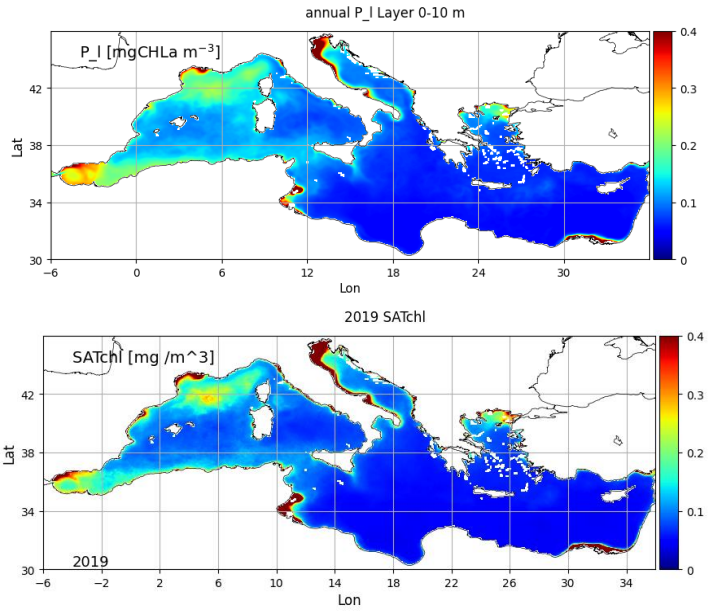

Figure 1.1. Mean model (top) and satellite (bottom) chlorophyll concentration.

Type of ocean area	Satellite - EANs			
	[mg/m³]		[Log(mg/m³)]	
	win	sum	win	sum
Open sea	0.06	0.01	0.16	0.07
Coastal	0.30	0.27	0.23	0.22

Layer [m]	BGC-Argo [mg/m³]	BGC-Argo	
0-10	0.06	**Average 0-200 m [mg/m³]**	0.03
10-30	0.06		
30-60	0.07	**Depth of DCM [m]**	8
60-100	0.06		
100-150	0.04	**Depth of WBL [m]**	27
EAN	0.06		

Table 1.1. Chlorophyll metrics. Reference dataset for comparison is reported in column titles.

2. Net Primary Production

Net primary production (NPP) is the measure of the net uptake of carbon by phytoplankton groups (gross primary production minus fast release processes – e.g., respiration). The lack of any extensive dataset of measures of primary production prevents the application of quantitative metrics for the assessment of the quality of this product. Thus, the product quality consists in a qualitative assessment of the consistency of the modelled NPP in 2019 with previous estimates published in scientific literature (Fig. 2.1 and Tab. 2.1). Averaged NPP in the different sub-basins are consistent with sub-basin estimations.

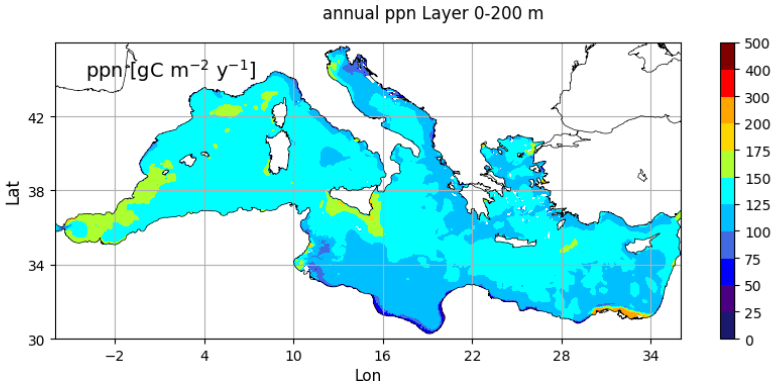

Figure 2.1. Net primary production integrated in the 0-200 m depth in the period 1999-2019.

	MODEL (Lazzari et al., 2012)	**SATELLITE** (Colella, 2006)	**IN-SITU ESTIMATES** (Siokou-Frangou et al., 2010)		**CMEMS A&F 2019**
	Annual mean [gC/m^2/y]		**Annual mean [gC/m^2/y]**	**Short term estimates [mgC/m^3/d]**	**Annual mean [gC/m^2/y]**
Mediterranean Sea	98 ±82	90 ±48			129
Alboran Sea	274 ±155	179 ±116		353–996; May-Jun1996 142; Nov2003	150
South West Med –West	160 ±89	113 ±43		186–636 (avg. 440) Oct1996	143
South West Med –East	118 ±70	102 ±38			137
North West Med	116 ±79	115 ±67	105.8-119.6 86-232 (only DYFAMED station) 140-170 (South Gulf of Lion)	353–996; May–Jun1996 401; Mar-Apr1998 (G. Lion) 166; Jan-Feb1999 (G. Lion) 160–760; May-Jul (Cat-Bal) 150–900; Apr1991 (Cat-Bal) 450, 700; Jun1993 (Cat-Bal) 210, 250; Oct1992 (Cat-Bal) 1000±71 Mar1999 (Cat-Bal) 404±248 Jan-Feb00 (Cat-Bal)	140
Levantine	76 ±61	72 ±21	59 (Cretan Sea)		127
Ionian Sea	77 ±58	79 ±23	61.8	119–419; May-June 1996 208–324; April-May 1999 186±65; August 1997-98	122
Tyrrhenian Sea	92 ±5	90 ±35		398; May–Jun1996 273; Jul2005 429; Dec2005	127

Table 2.1. Annual averages and short period estimates of the vertically integrated primary production for some selected sub-regions.

3. Phytoplankton biomass

The phytoplankton biomass is the content of carbon (mgC/m^3) in phytoplankton cells. The BFM model, featured by the MedBFM model system, simulated 4 phytoplankton functional groups and variable chlorophyll to carbon ratio, which depends on photoacclimatation and balance between synthesis and loss terms (Lazzari et al., 2012). Thus, phytoplankton biomass along with chlorophyll should be accounted for studying the evolution and variability of the primary producer biomass.

The accuracy of the phytoplankton biomass is assessed by class4 metrics using BGC-Argo optical data available in 2019. Observations for biomass of phytoplankton (PhytoC) are retrieved from particulate backscattering coefficient at 700 nm (bbp700) data using Bellacicco et al. (2019) relationship. Statistics computed for the comparison of vertical profiles (Table 3.1) show that the 0-200 m averaged values are reproduced with an accuracy of around 1.33 mgC/m^3 over mean values ranging from 4 to 7 mgC/m^3 for the vertical averaged phytoplankton biomass. The uneven distribution of BGC-Argo floats (i.e., only in open sea areas and some subbasins) limits the effectiveness of this comparison.

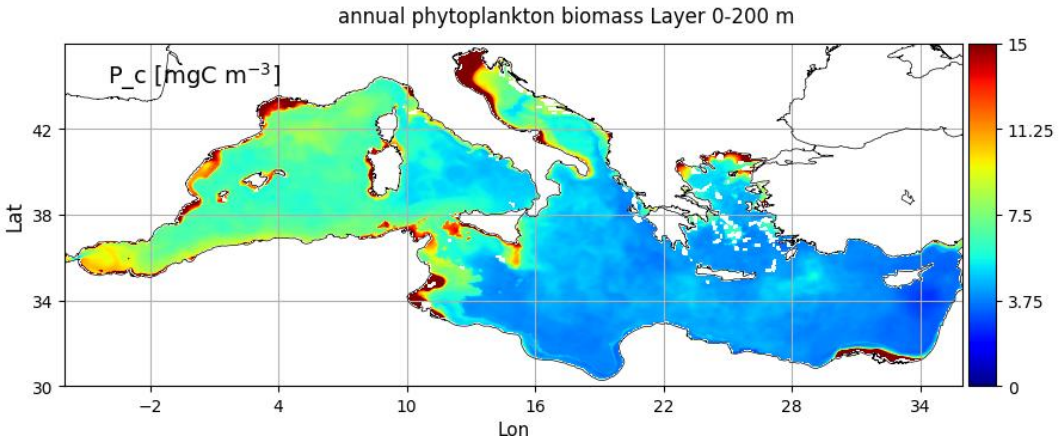

Figure 3.1. Average phytoplankton biomass at the 0-200 m layer in 2019.

Subbasin	Model mean average 0-200 m [mgC/m^3] for the BGC-Argo locations	RMSD with respect to BGC-Argo [mgC/m^3] of 0-200 m average
Swm	3.98	0.90
Nwm	6.95	3.00
Tyr	5.03	1.12
Adr	2.91	0.76
Ion	3.97	0.75
Lev	3.78	1.42
		MED average (EAN) 1.33

Table 3.1. Average phytoplankton biomass in the 0-200 m layer and its RMSD with respect to BGC-Argo floats.

4. Zooplankton biomass

Zooplankton biomass expressed as carbon represents the sum of the carbon content of the four zooplankton functional groups of the model. Due to the lack of extensive dataset of measurements of zooplankton, the product validation consists in a qualitative assessment of the consistency of the modelled zooplankton biomass in 2019 with measurements published in scientific literature. The model satisfactory simulated the order of magnitude of the variable (i.e., in the range of 0.5-1.3 gC/m^2) and the basin wide gradient with higher values in the western subbasins and lower values in the eastern ones (Tab. 4.1).

Model sub-basin	Heterotrophic Nanoflagelates [gC/m^2] in layer 0-200 m		Microzooplankton [gC/m^2] in layer 0-200 m		Mesozooplankton [gC/m^2] in layer 0-200m		Model Total carbon biomass of Zooplankton [gC/m^2] in layer 0-200 m
ALB					0.26	Apr [e]	1.25 ±0.21
					0.72;0.5****	Winter/spring [c]	
SWM1					1.45***	Jun [f]	1.17 ±0.17
SWM2	0.5	Jun/Jul [a]					1.17 ±0.15
NWM	0.88	Jun/Jul [a]	0.1-0.2*	May/Jun [d]	0.82±0.15	Apr [e]	1.12 ±0.16
	0.46-1.3** (NW Med current) 0.17-1.7** (NW offshore transect)	May/Jun [c]			0.9***	Jun [f]	
					0.58; 1.16; 1.6	different studies [c]	
					0.3;0.4;0.45****	Mar/Spring [c]	
TYR							0.91 ±0.16
ADR					0.30±00.05 0.15±00.02	Feb/Oct [e]	0.68 ±0.16
AEG	0.2* 0.8*	Mar/Sep [b]	0.16±0.04* 0.12±0.05*	Mar/Sep [b]	0.19±0.04* 0.16±0.04*	Mar/Sep [b]	0.64 ±0.14
					0.2 – 0.4****	Mar/Spring [c]	
ION	0.25 (western) 0.45 (southern) 0.40 (northern)	Jun/Jul [a]	0.02-0.28*	May/Jun [d]	Sicily channel 0.24±0.04 0.19±0.02	Mar/Sep [e]	0.72 ±0.16
					0.4****	Mar [c]	
					0.24±0.03 0.22±0.02	Mar/Aug [e]	
					0.95*** (eastern) 1.05*** (central) 0.85*** (central)	Jun [f]	
					0.4	Spring [c]	
LEV	0.25 (western) 0.26 (southern) 0.30 (Cyprus) 0.31 (Rhode gyre)	Jun/Jul [a]	0.08-0.12*	May/Jun [d]	0.44±0.26 (Rhode gyre) 0.20±0.02	Mar/Sep/Oct [e]	0.63±0.09
	0.23-0.52**	Sep [c]			0.7*** (rhode gyre) 0.4*** (south Cyprus) 0.65*** (MersaMatruh gyre)	Jun [f]	

*Table 4.1. Vertically integrated total carbon zooplankton biomass for selected sub-regions [gC/m^2]. Model total in the 0-200 m layer (last column). Data from: [a] Christaki et al. (2001); [b] Siokou-Frangou et al. (2002) (Southern Aegeran for layer 0-100 m); [c] Siokou-Frangou et al. (2010); [d] Dolan et al., (1999); [e] Mazzocchi et al., (2014); [f] Siokou et al., 2019. *data for 0-100 m; **data converted from abundance to biomass using 2.9 pg/ind (Cristaki et al., 2001); ***data converted from 0-1000 m to 0-200 m using the conversion factor of 0.75; ****dry weigh converted to biomass using the factor 4 grDW: 1 grC.*

5. Phosphate

The quality of phosphate product is assessed by skill performance statistics computed using climatological values and the corresponding model annual means for 2019 (Tab. 5.1). The climatological values (EMODnet2018_int) are based on the EMODnet dataset (Buga et al., 2018) and other scientific cruises listed in Cossarini et al. (2015) and Lazzari et al. (2016). The dataset spans the period 1997-2016. The Med-MFC phosphate product has a good accuracy in reproducing the average values and shape of the profiles along the Mediterranean sub-basins. On average, phosphate RMSD is 0.03 mmol/m^3 in the upper layers and ranges between 0.03 and 0.05 mmol/m^3 in the layers below 60 m (Tab. 5.1). The results enforce the good performance of the MedBFM model in reproducing the negative gradient from the western to the eastern sub-basins of the subsurface layers (correlation values higher than 0.7 below 30 m). Low phosphate values in the surface layer affect the model capability to clearly reproduce the west-to-east gradient, thus the correlation value is low.

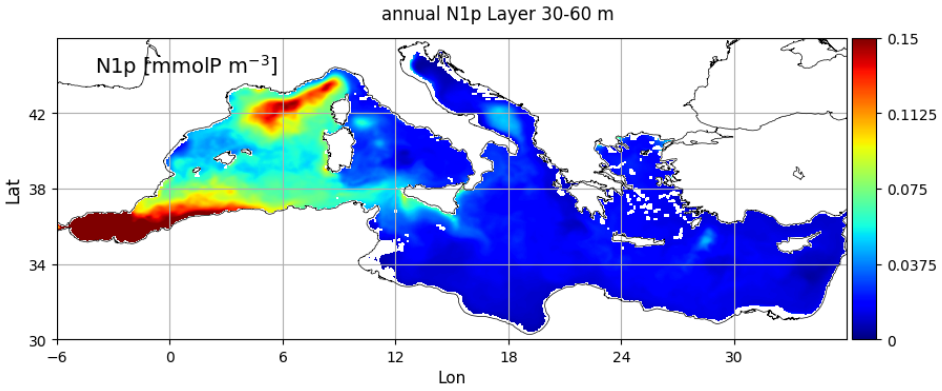

Figure 5.1. Model mean annual phosphate concentration in 2019 at layer 30-60 m [mmol/m^3].

Layer [m]	BIAS [mmol/m^3]	RMSD - EAN [mmol/m^3]	CORR
0-10	-0.01	0.03	0.32
10-30	0.00	0.03	0.27
30-60	0.00	0.03	0.72
60-100	0.00	0.03	0.92
100-150	0.03	0.05	0.89
150-300	0.03	0.04	0.97
300-600	-0.03	0.04	0.99
600-1000	-0.02	0.03	0.98

Table 5.1. Skill metrics (BIAS, RMSD and correlation) for the comparison of phosphate (model outputs averaged over the sub-basins and the period January – December 2019) with respect to climatology in open sea (EMODnet2018_int dataset).

6. Nitrate

The quality of nitrate product is assessed in a two-phase quantitative comparison: i) using EMODnet2018_int vertical climatological profiles (Sec. 5); ii) with BGC-Argo floats data available in 2019. The Med-MFC nitrate product has a good accuracy in reproducing the average values and shape of the climatological: on average, the RMSD of nitrate is 0.5 mmol/m^3 in the upper layers and around 0.8 mmol/m^3 in the layers below 60 m (Tab. 6.1). Together with phosphate ones, nitrate results corroborates the good performance of the MedBFM model in reproducing the deepening of the nutricline and the decreasing concentration values in the deep layers from the western to the eastern sub-basins. Low nitrate values in the surface layer affect the model capability to clearly reproduce the west-to-east gradient. Nitrate validation benefits from the availability of BGC-Argo floats data (Tab. 6.1), even if the number of BGC-Argo floats mounting a nitrate sensor is smaller than that for chlorophyll. Since MedBFM version at Q2/2020, the system assimilates nitrate BGC-Argo profiles (which generally has weekly frequency) and the comparison is performed using misfits. The misfit can be influenced by the assimilation of the same BGC-Argo float occurred in a position 50-150 km far for the present location one week before Nevertheless, the comparison of modelled nitrate with the BGC-Argo float data evaluates not only the accuracy of nitrate values (i.e., RMSD for selected layers) but also the consistency of the MedBFM to simulate key coupled physical-biogeochemical processes (i.e., water column nutrient content, nitracline and effect of winter mixing and summer stratification on the shape of nitrate profile). Our validation framework shows that the MedBFM model system has a good performance in simulating the shape of profiles and the seasonal evolution of the mesoscale dynamics: the mean value of nitrate on the 0-200 m layer is simulated with an accuracy of about 0.22 mmol/m^3 and the nitracline depth with a mean uncertainty of 13 m (Tab. 6.1).

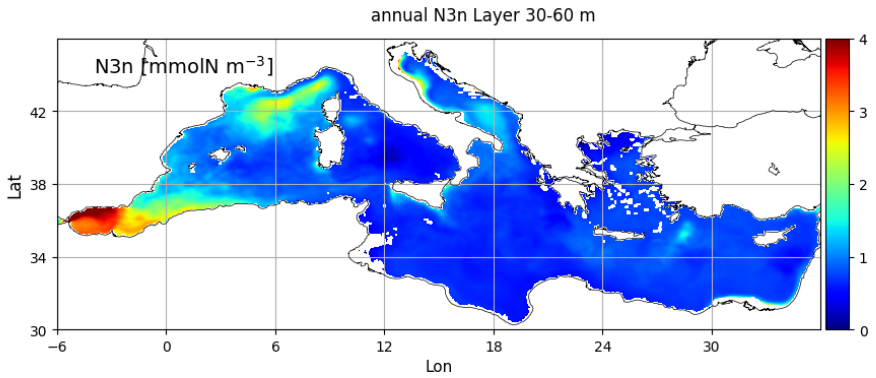

Figure 6.1. Model mean annual nitrate concentration in 2019 at layer 30-60 m [mmol/m^3].

Layer [m]	RMSDs			
	EMODnet2018_int EAN [mmol/m^3]	BGC-Argo [mmol/m^3]	BGC-Argo	
0-10	0.51	0.44	**Mean nitrate concentration 0-200 m [mmol/m^3]**	0.22
10-30	0.59	0.42		
30-60	0.66	0.46		
60-100	0.73	0.44		
100-150	0.97	0.39	**Depth of the nitracline [m]**	13
150-300	0.69	0.30		
300-600	0.89	0.27		
600-1000	0.68	0.78		

Table 6.1. Validation metrics of nitrate. Reference dataset for comparison is reported in column titles.

7. Dissolved Oxygen

The quality of CMEMS Med-MFC dissolved oxygen is assessed in a two-phase quantitative comparison: i) using EMODnet2018_int vertical climatological profiles (Sec. 5); ii) with BGC-Argo floats data available in 2019. Modelled oxygen profiles are well simulated within the range of variability of the climatology with RMSDs lower than 7 mmol/m^3 in all selected layers, with the exception of layer 100-150 m (Tab. 7.1).

The validation of dissolved oxygen benefits from the availability of BGC-Argo float data. Since MedBFM version at Q4/2022, the system assimilates oxygen BGC-Argo profiles, and the comparison is performed using misfits. Given the frequency of BGC-Argo data is generally weekly, the misfit can be influenced by the assimilation of the same BGC-Argo float occurred in a position 50-150km far from the present location one week before (i.e., BGC-Argo float should be considered as semi-independent data).

RMSD with respect to BGC-Argo is lower than 5 mmol/m^3 in the surface layer (down to 30 m). Slightly higher uncertainty is computed for the deeper layers with RMSD values ranging between 4 and 6 mmol/m^3.

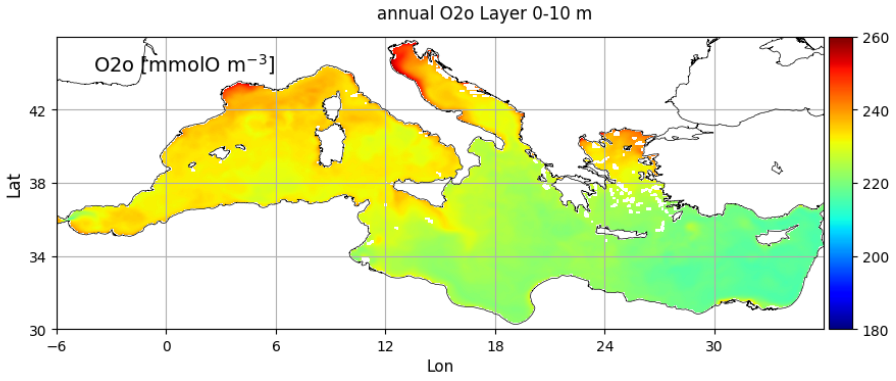

Figure 7.1. Model mean annual phosphate concentration in 2019 at layer 0-10 m [mmol/m^3].

Layer [m]	RMSDs [mmol/m^3]	
	EMODnet2018_int EAN	BGC-Argo
0-10	5.5	3.8
10-30	5.2	4.5
30-60	5.6	6.3
60-100	3.8	5.7
100-150	6.1	5.5
150-300	5.7	4.6
300-600	6.9	4.0
600-1000	6.0	5.3

Table 7.1. Validation metrics of dissolved oxygen. Reference dataset for comparison is reported in column titles.

8. Ammonium

Ammonium accuracy is assessed with Class 1 metrics: it consists in the comparison between model average vertical profiles for 2019 and the EMODnet2018_int reference climatological profiles (Sec. 5). As reported in Table 8.1, ammonium concentrations are simulated by the MedBFM model with an error of less than 0.4 mmol/m^3 in the upper layers and of 0.3-0.6 mmol/m^3 in the deeper layers (i.e., between 100 and 600 m). The low and negative correlation values indicate that the model has some deficiencies in reproducing typical vertical profiles and spatial gradient of ammonium, however the low data availability (only 7 sub-basins covered) might have affected the accuracy evaluation.

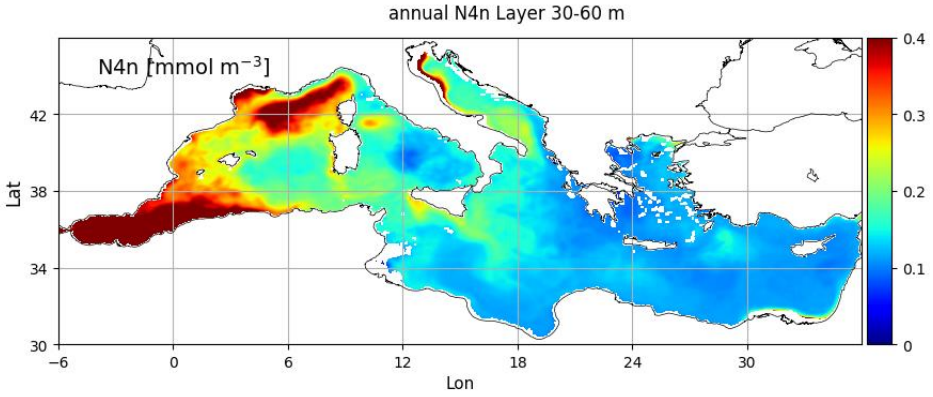

Figure 8.1. Model mean annual ammonium concentration in 2019 at layer 30-60 m [mmol/m^3].

Layer depth [m]	BIAS [mmol/m^3]	RMSD - EAN [mmol/m^3]	CORR
0-10	-0.33	0.38	-0.14
10-30	-0.14	0.19	-0.16
30-60	-0.06	0.15	-0.08
60-100	-0.03	0.24	-0.44
100-150	-0.10	0.31	-0.41
150-300	-0.22	0.32	-0.26
300-600	-0.37	0.43	0.77
600-1000	-0.40	0.55	0.84

Table 8.1. Skill metrics (BIAS, RMSD and correlation) for the comparison of ammonium (model outputs averaged over the sub-basins and the period January – December 2019) with respect to climatology in open sea (EMODnet2018_int dataset).

9. Silicate

Silicate validation is performed with Class 1 metrics assessment: it consists in the comparison between model average vertical profiles for 2019 and the EMODnet2018_int reference climatological profiles (Sec. 5). As reported in Table 9.1, silicate concentrations are simulated by the MedBFM model with an uncertainty below of 0.7 mmol/m^3 in the upper layers and of about 0.5-0.8 mmol/m^3 in the deeper layers (i.e., below 60 m). Low correlation value in the surface layer indicates that the model has some deficiencies in reproducing the typical surface spatial gradient of silicate concentration, that occurs especially in the western basin. The correlation values of the deep layers are pretty high (around 0.8) highlighting that subsurface modelled gradients are consistent with observations.

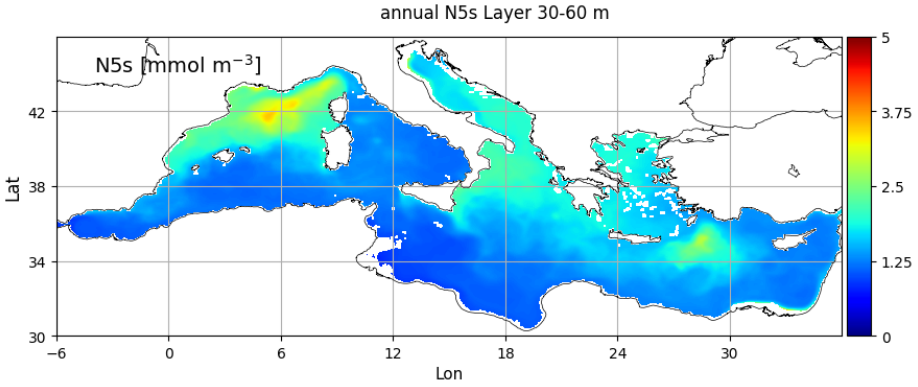

Figure 9.1. Model mean annual silicate concentration in 2019 at layer 30-60 m [mmol/m^3].

	Silicate		
Layer depth [m]	**BIAS [mmol/m^3]**	**RMSD [mmol/m^3]**	**CORR**
0-10	0.59	0.65	0.77
10-30	0.63	0.69	0.71
30-60	0.49	0.55	0.78
60-100	0.35	0.51	0.74
100-150	0.57	0.81	0.62
150-300	0.56	0.83	0.73
300-600	-0.48	0.72	0.89
600-1000	-0.43	0.65	0.93

Table 9.1. Skill metrics (BIAS, RMSD and correlation) for the comparison of silicate (model outputs averaged over the sub-basins and the period January – December 2019) with respect to climatology in open sea (EMODnet2018_int dataset).

10. pH

The sea water acidity is expressed by the pH in total scale at in situ conditions. pH validation is performed with Class 1 metrics assessment: it consists in the comparison between model average vertical profiles for 2019 and the EMODnet2018_int reference climatological profiles (Sec. 5). The comparison shows the good skill of the model in representing the basin-wide gradient and sub-basin vertical pH profiles. The statistics computed using the 16 sub-basins climatological values and the corresponding model annual means (Tab. 10.1) highlights that uncertainty, which never exceeds 0.04, is lower in the deeper layers than at surface.

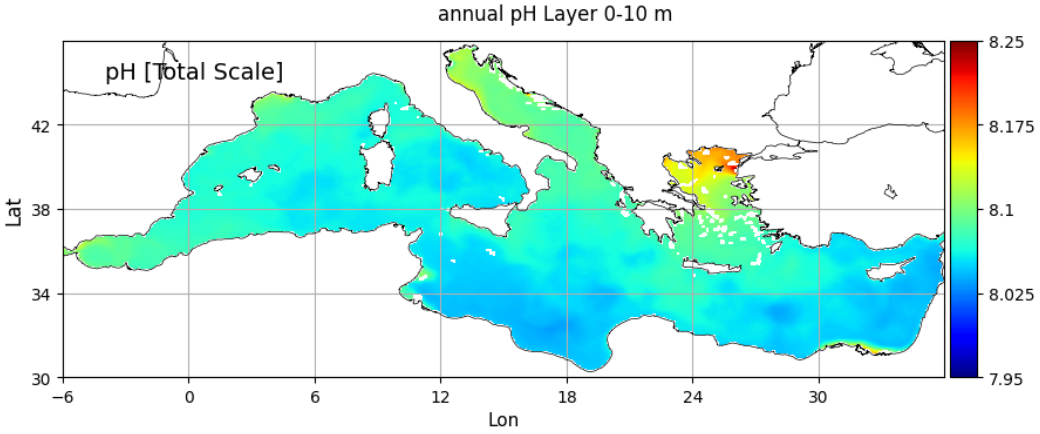

Figure 10.1. Model mean annual pH in total scale in 2019 at layer 0-10 m.

Layer depth [m]	BIAS	RMSD - EAN	CORR
0-10	-0.012	0.032	0.78
10-30	-0.011	0.023	0.68
30-60	-0.016	0.028	0.43
60-100	-0.001	0.025	0.66
100-150	0.008	0.017	0.78
150-300	0.006	0.014	0.92
300-600	0.012	0.014	0.97
600-1000	0.004	0.007	0.97

Table 10.1. Skill metrics (BIAS, RMSD and correlation) for the comparison of pH in total scale (model outputs averaged over the sub-basins and the period January – December 2019) with respect to climatology in open sea (EMODnet2018_int dataset).

11. Alkalinity

The validation of the Alkalinity (ALK) is performed with Class 1 metrics assessment: it consists in the comparison between model average vertical profiles for 2019 and the EMODnet2018_int reference climatological profiles (Sec. 5). It is worth to note that alkalinity is typically reported as μmol/kg whereas the Marine Copernicus product is reported as mol/m^3. The density of seawater is needed for the conversion. The profiles are well simulated within the range of variability of the climatology except in the western basins where the model overestimates concentration of alkalinity at the surface. As reported in Tab. 11.1, alkalinity concentrations are simulated by the MedBFM model with an error of around 40 μmol/kg in the upper layers and of about 10-20 μmol/kg in the deeper layers (i.e., below 60 m). High correlation values in all layers indicate that the model reproduces the typical spatial gradient of alkalinity.

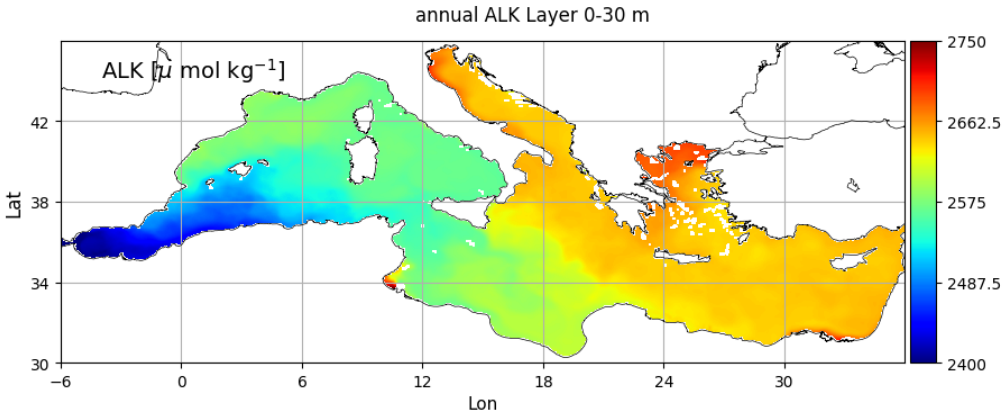

Figure 11.1. Model mean annual alkalinity in 2019 at layer 0-300 m [μmol/m^3].

Layer depth [m]	BIAS [μmol/kg]	RMSD - EAN [mmol/kg]	CORR
0-10	22.61	39.25	0.93
10-30	21.69	29.88	0.97
30-60	16.48	22.70	0.98
60-100	6.24	18.93	0.94
100-150	8.73	10.22	0.99
150-300	1.55	13.49	0.93
300-600	0.50	9.89	0.89
600-1000	-0.09	8.27	0.93

Table 11.1. Skill metrics (BIAS, RMSD and correlation) for the comparison of alkalinity (model outputs averaged over the sub-basins and the period January – December 2019) with respect to climatology in open sea (EMODnet2018_int dataset).

12. Dissolved inorganic carbon

The validation of dissolved inorganic carbon (DIC) is performed with Class 1 metrics assessment: it consists in the comparison between model average vertical profiles for 2019 and the EMODnet2018_int reference climatological profiles (Sec. 5). It is worth to note that DIC is typically reported as μmol/kg whereas the Marine Copernicus product is reported as mol/m^3. The density of seawater is needed for the conversion. As reported in Tab. 12.1, DIC concentrations are simulated by the MedBFM model with an error of around 40 μmol/kg in the upper layers and of about 4-16 μmol/kg in the deeper layers (i.e., below 60 m). High correlation values in all layers indicate that the model reproduces the typical spatial gradient of DIC. It is worth to note that higher uncertainty of DIC and alkalinity is associated with high variability of the two variables in the upper layers (down to 60 m), whereas deeper values remain almost constant during the year. This high variability at the surface of DIC and also ALK dynamics is determined by three major factors: the input in the eastern marginal seas (the terrestrial input from the Po and other Italian rivers and the input from the Dardanelles), the effect of evaporation in the eastern basin (which has a seasonal component), and the influx of the low-ALK and low-DIC Atlantic waters in the western basin.

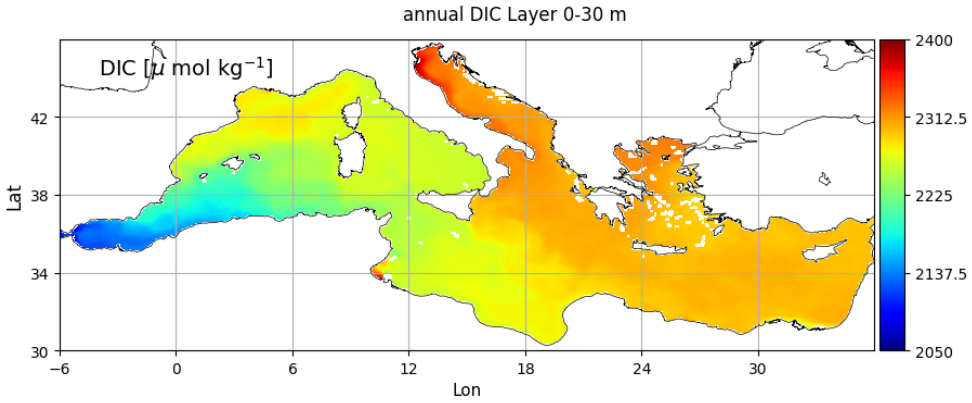

Figure 12.1. Model mean annual dissolved inorganic carbon in 2019 at layer 0-300 m [μmol/m^3].

Layer [m]	BIAS [μmol/kg]	RMSD - EAN [μmol/kg]	CORR
0-10	22.2	34.0	0.93
10-30	24.3	30.6	0.95
30-60	17.0	24.1	0.93
60-100	4.5	16.4	0.88
100-150	0.8	14.3	0.87
150-300	-2.8	8.2	0.82
300-600	-7.4	11.0	0.79
600-1000	-1.6	4.1	0.93

Table 12.1. Skill metrics (BIAS, RMSD and correlation) for the comparison of DIC (model outputs averaged over the sub-basins and the period January – December 2019) with respect to climatology in open sea (EMODnet2018_int dataset).

13. Surface partial pressure of CO2

Two reference datasets are used for the validation of surface pCO2 modelled for 2019: one of in situ or recalculated pCO2 values derived from the EMODnet2018_int dataset (Sec. 5) and the dedicated global dataset SOCAT v2 of pCO2 measurements. Climatological reference monthly values are derived from the SOCAT dataset and compared with the modelled seasonal cycle for 2019 (Fig. 13.1). Class 1 metrics validation are summarized in Table 13.1. The model overestimation (and error) is due to the fact that the two climatologies refer to a past condition (observations from the 2000-2015 period). Thus, the current trend of surface pCO2 simulated by the model is not fully accounted for in the reference datasets. The lack of NRT observations represents a limit for an accurate validation of this variable. To be finalized

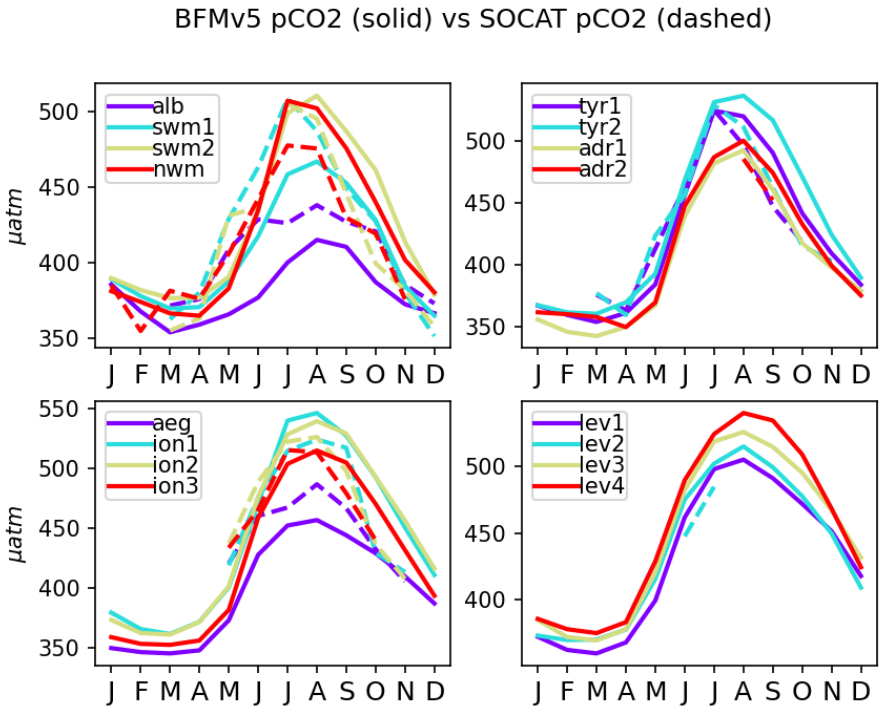

Figure 13.1. Model (solid lines) mean seasonal cycle of surface partial pressure of CO_2 [µatm] in 2019 compared with the Socat dataset (dotted lines).

Dataset	Surface pCO2 [µatm]		
	BIAS	RMSD	CORR
EMODnet2018; pCO2 at 0-10 m	16.6	36.0	0.69
SOCAT v2; surface pCO2	35.7	42.4	0.91

Table 13.1 *Skill metrics for the comparison of surface pCO2 with respect to sub-basin climatology in open sea.*

14. Surface flux of CO2

The modelled mean annual CO2 air-sea flux (Fig. 14.1) for 2019 can be qualitatively compared with previous published estimations (section 1.7 of the Ocean State Report in Schuckmann et al., 2018; D'Ortenzio et al., 2008; Melaku Canu et al., 2015). The mean annual patterns, i.e. western-to-eastern and northern-to-southern decreasing gradients and the almost neutral conditions, are in agreement with the previous estimations. The west to east gradient of the air-sea CO2 flux simulated by the model in the operational configuration in 2019 is consistent with the reanalysis product presented in the Ocean State Report, even if values tend to be mostly positive in the 2019 simulation (sink flux from the atmosphere to the sea). To be finalized

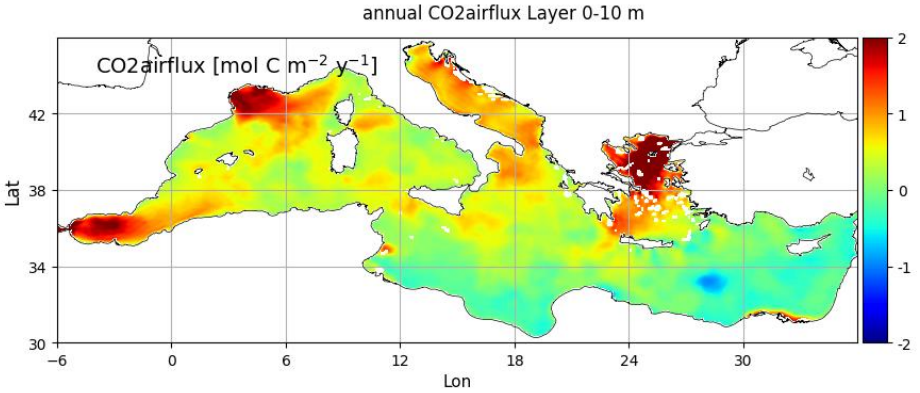

Figure 14.1. Model mean annual map for 2019 of surface flux of CO2 [mol C m^{-2} y^{-1}].

15. Light attenuation coef. at 490 nm (Kd490)

Modelled diffuse attenuation coefficient for downwelling irradiance at the 490nm wavelength is compared with the Marine Copernicus Ocean Color MED_CHL_L3_REP_OBSERVATIONS_009_078 products. Statistics, which are computed for each of the 16 sub-basins, are summarized in Table 15.1 for the winter and summer periods.

The highest uncertainty values are in the western sub-basins in winter.

Light attenuation coefficient Kd490 [m^{-1}]				
	RMSD		**BIAS**	
	win	**sum**	**win**	**sum**
OPEN SEA				
Mod-Sat	0.008	0.006	-0.001	0.005
log_{10}(Mod)-log_{10}(Sat)	0.073	0.086	-0.001	0.078

Table 15.1 *Mean RMSD and BIAS (model minus satellite) of surface light attenuation coefficient at the 490 nm wavelength (Kd490, [m^{-1}]) chlorophyll [mg m^{-3}] over the open sea and coastal areas of the Mediterranean Sea. Winter corresponds to January to April, summer corresponds to June to September.*

16. Phytoplankton Functional Types (PFTs)

Model PFTs (Diatoms, Nanoflagellates, Picophytoplankton and Dinoflagellates) are compared with in situ data and a PFTs product derived from satellite (OCEANCOLOUR_MED_BGC_L3_MY_009_143). The Model reproduces quite well the in situ PFTs profiles and seasonal cycle, excepting nanoflagellates that shows a higher RMSDs and general model underestimation. The visual comparison of the model results with the satellite-derived PFTs shows that model and satellite estimates have the same temporal and spatial patterns with dominance of picophytoplankton in the summer period.

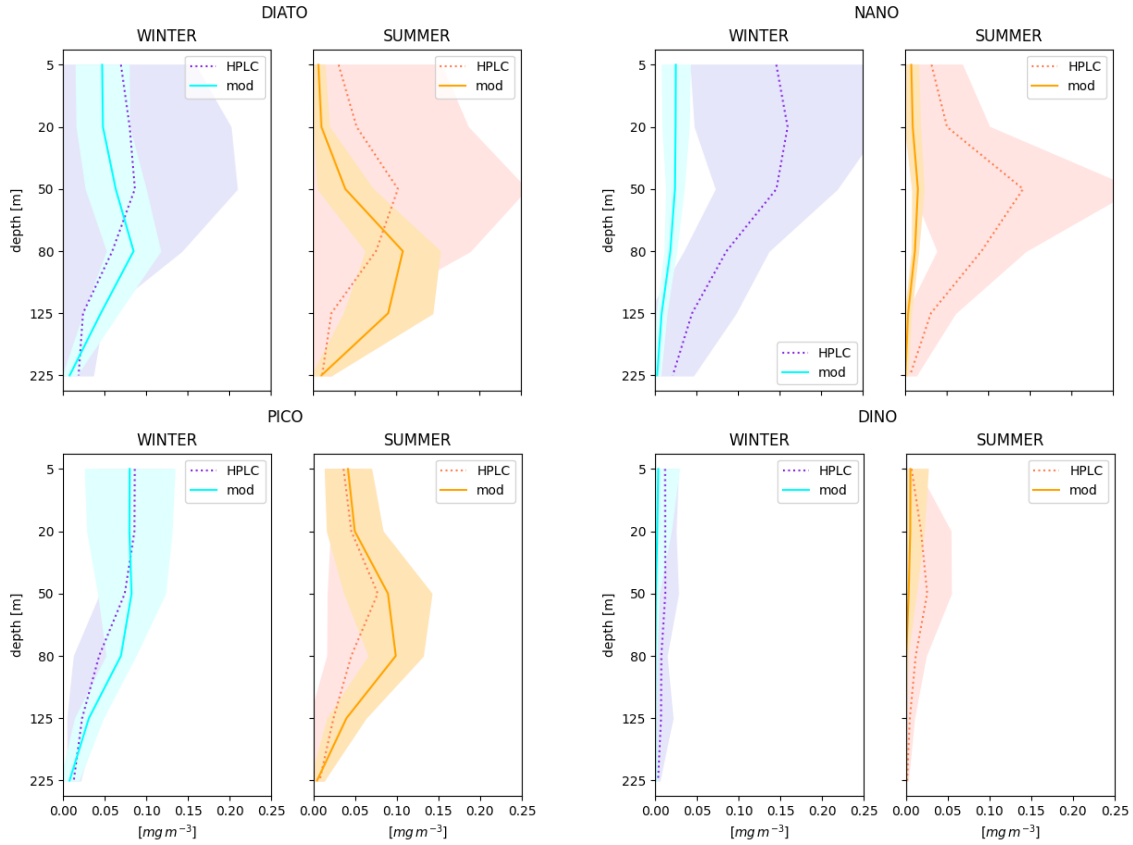

*Figure 16.1. climatological winter and summer profiles of the 4 PFTs for **mod**el (solid line) and HPLC data (dashed line) and the relative spatial STD in shading. DIATO: Diatoms, NANO: Nanoflagellates, PICO: Picophytoplankton, and DINO: Dinoflagellates.*

Layer depth [m]	DIATO		NANO		PICO		DINO	
	Win	sum	win	sum	win	sum	win	sum
0-10	0.06	0.03	0.12	0.02	0.05	0.01	0.01	0.01
10-30	0.08	0.04	0.14	0.03	0.05	0.02	0.01	0.03
30-60	0.09	0.06	0.13	0.13	0.04	0.03	0.01	0.03
60-100	0.08	0.08	0.07	0.11	0.03	0.06	0.01	0.01
100-150	0.04	0.08	0.04	0.03	0.02	0.02	0.01	0.01
150-300	0.01	0.01	0.02	0.01	0.01	0.01	0.00	0.00
EANs	0.07	0.06	0.10	0.06	0.04	0.03	0.01	0.02

***Table 16.1** Winter and summer mean RMSD [mg/m³] calculated on the aggregated sub-basins for the 4 PFTs with respect to HPLC data for selected layers in the euphotic zone.*

References

Bellacicco, M., Vellucci, V., Scardi, M., Barbieux, M., Marullo, S., D'Ortenzio, F., 2019. Quantifying the Impact of Linear Regression Model in Deriving Bio-Optical Relationships: The Implications on Ocean Carbon Estimations. Sensors 19, 3032. https://doi.org/10.3390/s19133032

Bittig, H.C., Maurer, T.L., Plant, J.N., Schmechtig, C., Wong, A.P.S., Claustre, H., Trull, T.W., Udaya Bhaskar, T.V.S., Boss, E., Dall'Olmo, G., Organelli, E., Poteau, A., Johnson, K.S., Hanstein, C., Leymarie, E., Le Reste, S., Riser, S.C., Rupan, A.R., Taillandier, V., Thierry, V., Xing, X., 2019. A BGC-Argo Guide: Planning, Deployment, Data Handling and Usage. Front. Mar. Sci. 6. https://doi.org/10.3389/fmars.2019.00502

Buga, L., Sarbu, G., Fryberg, L., Magnus, W., Wesslander, K., Gatti, J., Leroy, D., Iona, S., Larsen, M., Koefoed Rømer, J., Østrem, A.K., Lipizer, M., Giorgietti, A., 2018. EMODnet Chemistry Eutrophication and Acidity aggregated datasets v2018. https://doi.org/10.6092/EC8207EF-ED81-4EE5-BF48-E26FF16BF02E

Colella, S. 2006. La produzione primaria nel Mar Mediterraneo da satellite: sviluppo di un modello regionale e sua applicazione affidati SeaWiFS, MODIS e MERIS, PhD Thesis, Università degli studi di Napoli "Federico II".

Cossarini, G., Lazzari, P., Solidoro, C., 2015. Spatiotemporal variability of alkalinity in the Mediterranean Sea. Biogeosciences 12, 1647–1658. https://doi.org/10.5194/bg-12-1647-2015

D'Ortenzio, F., Antoine, D., Marullo, S., 2008. Satellite-driven modeling of the upper ocean mixed layer and air–sea CO2 flux in the Mediterranean Sea. Deep Sea Res. Part Oceanogr. Res. Pap. 55, 405–434. https://doi.org/10.1016/j.dsr.2007.12.008

Hernandez, F., Smith, G., Baetens, K., Cossarini, G., Garcia-Hermosa, I., Drevillon, M., Maksymczuk, J., Melet, A., Regnier, C., von Schuckman, K., 2018. Measuring Performances, Skill and Accuracy in Operational Oceanography: New Challenges and Approaches, in: Chassignet, E.P., Pascual, A., Tintoré, J., Verron, J. (Eds.), New Frontiers in Operational Oceanography. CreateSpace Independent Publishing Platform, pp. 759–795.

Lazzari, P., Solidoro, C., Ibello, V., Salon, S., Teruzzi, A., Béranger, K., Colella, S., Crise, A., 2012. Seasonal and inter-annual variability of plankton chlorophyll and primary production in the Mediterranean Sea: a modelling approach. Biogeosciences 9, 217–233. https://doi.org/10.5194/bg-9-217-2012

Lazzari, P., Solidoro, C., Salon, S., Bolzon, G., 2016. Spatial variability of phosphate and nitrate in the Mediterranean Sea: A modeling approach. Deep Sea Res. Part Oceanogr. Res. Pap. 108, 39–52. https://doi.org/10.1016/j.dsr.2015.12.006

Melaku Canu, D., Ghermandi, A., Nunes, P.A.L.D., Lazzari, P., Cossarini, G., Solidoro, C., 2015. Estimating the value of carbon sequestration ecosystem services in the Mediterranean Sea: An ecological economics approach. Glob. Environ. Change 32, 87–95. https://doi.org/10.1016/j.gloenvcha.2015.02.008

Schuckmann, K. von, Traon, P.-Y.L., Smith, N., Pascual, A., Brasseur, P., Fennel, K., Djavidnia, S., Aaboe, S., Fanjul, E.A., Autret, E., Axell, L., Aznar, R., Benincasa, M., Bentamy, A., Boberg, F., Bourdallé-Badie, R., Nardelli, B.B., Brando, V.E., Bricaud, C., Breivik, L.-A., Brewin, R.J.W., Capet, A., Ceschin, A., Ciliberti, S., Cossarini, G., Alfonso, M. de, Collar, A. de P., Kloe, J. de, Deshayes, J., Desportes, C., Drévillon, M., Drillet, Y., Droghei, R., Dubois,

C., Embury, O., Etienne, H., Fratianni, C., Lafuente, J.G., Sotillo, M.G., Garric, G., Gasparin, F., Gerin, R., Good, S., Gourrion, J., Grégoire, M., Greiner, E., Guinehut, S., Gutknecht, E., Hernandez, F., Hernandez, O., Høyer, J., Jackson, L., Jandt, S., Josey, S., Juza, M., Kennedy, J., Kokkini, Z., Korres, G., Kõuts, M., Lagemaa, P., Lavergne, T., Cann, B. le, Legeais, J.-F., Lemieux-Dudon, B., Levier, B., Lien, V., Maljutenko, I., Manzano, F., Marcos, M., Marinova, V., Masina, S., Mauri, E., Mayer, M., Melet, A., Mélin, F., Meyssignac, B., Monier, M., Müller, M., Mulet, S., Naranjo, C., Notarstefano, G., Paulmier, A., Gomez, B.P., Gonzalez, I.P., Peneva, E., Perruche, C., Peterson, K.A., Pinardi, N., Pisano, A., Pardo, S., Poulain, P.-M., Raj, R.P., Raudsepp, U., Ravdas, M., Reid, R., Rio, M.-H., Salon, S., Samuelsen, A., Sammartino, M., Sammartino, S., Sandø, A.B., Santoleri, R., Sathyendranath, S., She, J., Simoncelli, S., Solidoro, C., Stoffelen, A., Storto, A., Szerkely, T., Tamm, S., Tietsche, S., Tinker, J., Tintore, J., Trindade, A., Zanten, D. van, Vandenbulcke, L., Verhoef, A., Verbrugge, N., Viktorsson, L., Schuckmann, K. von, Wakelin, S.L., Zacharioudaki, A., Zuo, H., 2018. Copernicus Marine Service Ocean State Report. J. Oper. Oceanogr. 11, S1–S142. https://doi.org/10.1080/1755876X.2018.1489208

Siokou-Frangou, I., Christaki, U., Mazzocchi, M.G., Montresor, M., Ribera d'Alcalá, M., Vaqué, D., Zingone, A., 2010. Plankton in the open Mediterranean Sea: a review. Biogeosciences 7, 1543–1586. https://doi.org/10.5194/bg-7-1543-2010